

Nonlinear and perturbative evolution of distorted black holes: Odd-parity modes

John Baker, Steven Brandt, and Manuela Campanelli

Albert-Einstein-Institut, Max-Planck-Institut für Gravitationsphysik, Am Mühlenberg 1, D-14476 Golm, Germany

Carlos O. Lousto

*Albert-Einstein-Institut, Max-Planck-Institut für Gravitationsphysik, Am Mühlenberg 1, D-14476 Golm, Germany
and Instituto de Astronomía y Física del Espacio, Consejo Nacional de Investigaciones Científicas y Técnicas,
Buenos Aires, Argentina*

Edward Seidel

*Albert-Einstein-Institut, Max-Planck-Institut für Gravitationsphysik, Am Mühlenberg 1, D-14476 Golm, Germany
and National Center for Supercomputing Applications, Beckman Institute, 405 North Mathews Avenue, Urbana, Illinois 61801*

Ryoji Takahashi

Albert-Einstein-Institut, Max-Planck-Institut für Gravitationsphysik, Am Mühlenberg 1, D-14476 Golm, Germany

(Received 5 November 1999; revised manuscript received 24 August 2000; published 14 November 2000)

We study fully nonlinear and perturbative evolutions of nonrotating black holes with odd-parity distortions. Perturbative methods proved to be useful in order to interpret the nonlinear results. In particular, they provided insight on the nonlinear dependence of the wave forms with the distortion parameter Q_0 , explaining it in terms of the multipole coupling. We also found an increase in the frequency of the wave forms in the nonlinear regime which results from the loss of a noticeable part of the initial total mass of the system to gravitational radiation producing effectively a drifting of the quasinormal frequencies. The nonlinear evolutions have been performed (and cross checked) with the 3D parallel code for numerical relativity, CACTUS, and an independent axisymmetric code MAGOR. The linearized ones using the Regge-Wheeler formalism.

PACS number(s): 04.25.Dm, 04.30.Db, 95.30.Sf, 97.60.Lf

Coalescing black holes are considered one of the most promising sources of gravitational waves for gravitational wave observatories such as the Laser Interferometric Gravitational Wave Observatory (LIGO) and VIRGO-GEO-TAMA network under construction. Reliable wave form information about the merger of coalescing black holes can be crucial not only to the interpretation of such observations, but also could greatly enhance the detection rate. Numerical relativity is expected to provide a detailed theoretical understanding of the coalescence process.

There are at least two important ways in which a perturbative treatment can actually aid the numerical simulation. First, as shown in Ref. [1], it is possible to use perturbative evolutions to provide good outer boundary conditions for a numerical simulation, since away from the strong field region one expects to see low amplitude gravitational waves propagating on a black hole background. This information can be exploited in the outer region in providing boundary data. Second, this combined approach can be used in future applications of perturbative approaches to “take over” and continue a previously computed full scale nonlinear numerical simulation. For example, if gravitational wave forms are of primary interest in a simulation, once the system has evolved towards a perturbative regime (e.g., two coalescing black holes form a distorted Kerr hole, or evolve close enough that a close limit approximation is valid), then one may be able to extract the relevant gravitational wave data, and evolve them on the appropriate black hole background to extract wave forms [2]. As discussed above, 3D black hole evolutions using traditional ADM style formulations, with

singularity avoiding slicings, generally break down before complete wave forms can be extracted. A perturbative approach may be necessary in such cases to extract the relevant wave form physics.

All work to date in this area of comparing full scale numerical simulations with perturbative approaches has dealt with even-parity distortions of Schwarzschild-like black holes. See for instance Ref. [3], referred to here as paper I, where we compared perturbative techniques, based on the Zerilli approach, with fully nonlinear evolutions of even-parity distorted black holes. The more general black hole case has both even- and *odd*-parity distortions, and also involves black holes with angular momentum. Our starting point is represented by a distorted black hole initial data sets developed originally by Brandt and Seidel [4] to mimic the coalescence process. These data sets correspond to “arbitrarily” distorted rotating *single* black holes, such as those that will be formed in the coalescence of two black holes. Although this black hole family can include rotation, in this first step we restrict ourselves to the non-rotating limit (the so-called “odd-parity distorted Schwarzschild”). The details of this initial data procedure are covered in [4], so we will go over them only briefly here. We follow the standard 3+1 Arnowitt-Deser-Misner (ADM) decomposition of the Einstein equations which give us a spatial metric, an extrinsic curvature, a lapse and a shift. We choose our system such that we have a conformally flat three-metric γ_{ij} defined by

$$ds^2 = \Psi^4 (d\eta^2 + d\theta^2 + \sin^2\theta d\varphi^2), \quad (1)$$

where the coordinates θ and φ are the usual spherical coordinates.

dinates and the radial coordinate has been replaced by an exponential radial coordinate η [$\bar{r} = (M/2)e^\eta$].

The extrinsic curvature is chosen to be

$$K_{ij} = \Psi^{-2} h_{ij} = \Psi^{-2} \begin{pmatrix} 0 & 0 & H_E \\ 0 & 0 & H_F \\ H_E & H_F & 0 \end{pmatrix}, \quad (2)$$

where

$$H_E = q_G((n' + 1) - (2 + n') \sin^2 \theta) \sin^{n'-1} \theta, \quad (3)$$

$$H_F = -\partial_\eta q_G \cos \theta \sin^{n'} \theta, \quad (4)$$

$$q_G = Q_0 \left[\exp\left(-\frac{(\eta - \eta_0)^2}{\sigma^2}\right) + \exp\left(-\frac{(\eta + \eta_0)^2}{\sigma^2}\right) \right]. \quad (5)$$

The various functions have been chosen so that the momentum constraints are automatically satisfied, and have the form of odd-parity distortions in the black hole extrinsic curvature. The function q_G provides an adjustable distortion function, which satisfies the isometry operation, and whose amplitude is controlled by the parameter Q_0 . Since we will be comparing cases with different masses we will refer to an amplitude $\tilde{Q}_0 = Q_0/M^2$ normalized by the ADM mass of the initial slice. If Q_0 vanishes, an unperturbed Schwarzschild black hole results. The parameter n' is used to describe an ‘‘odd-parity’’ distortion. It must be odd, and have a value of at least 3. The function Ψ is the conformal factor, which we have abstracted from the metric and extrinsic curvature according to the factorization given by Lichnerowicz. This decomposition is valuable, because it allows us to solve the momentum and Hamiltonian constraints separately.

The theory of metric perturbations around a Schwarzschild hole was originally derived by Regge and Wheeler [5] for odd-parity perturbations and by Zerilli [6] for even-parity ones. The spherically symmetric background allows for a multipole decomposition even in the time domain. Moncrief [7] has given a gauge-invariant formulation of the problem, which like the work of Regge-Wheeler and Zerilli, is given in terms of the three-geometry metric perturbations. For special combinations of the perturbation equations, the famous Regge-Wheeler [5] wave equation, resulted for a single function $\phi_{(lm)}$:

$$-\frac{\partial^2 \phi_{(lm)}}{\partial t^2} + \frac{\partial^2 \phi_{(lm)}}{\partial r^{*2}} - V_l^-(r) \phi_{(lm)} = 0. \quad (6)$$

Because we are considering only axisymmetric perturbations all components with $m \neq 0$ vanish identically. We will subsequently suppress the m labels.

For the specific initial data given above we obtain

$$\phi_l|_{t=0} = 0, \quad (7)$$

$$\begin{aligned} \partial_t \phi_l|_{t=0} = & -\frac{2}{r^3} \left(1 - \frac{2M}{r}\right) \\ & \times \left\{ \frac{(4-l)}{(l-2)l(l+2)} q_G - \frac{(4-l)(l+1)}{(l-2)l} \right. \\ & \left. \times \left[\partial_\eta^2 q_G + \frac{(7M-3r)}{r \sqrt{1 - \frac{2M}{r}}} \partial_\eta q_G \right] \right\}. \quad (8) \end{aligned}$$

The 2D fully nonlinear evolutions have been performed with a code, MAGOR, designed to evolve axisymmetric, rotating, highly distorted black holes. In a nutshell, this nonlinear code solves the complete set of Einstein equations, in axisymmetry, with maximal slicing, for a rotating black hole. The code is written in a spherical-polar coordinate system, with the rescaled radial coordinate η that vanishes on the black hole throat. An isometry operator is used to provide boundary conditions on the throat of the black hole. All three components of a shift vector are employed to keep all off diagonal components of the metric zero, except for the $g_{\theta\phi}$ component, which carries information about the odd-parity polarization of the radiation. For more details of the code, see Ref. [4].

The last of our approaches for evolving these distorted black hole data sets utilizes full 3D nonlinear numerical relativity, and is based on CACTUS. For this paper, CACTUS was used to assemble a set of 3D initial data, evolution modules, and analysis routines needed for the comparisons with MAGOR and the perturbative approach described above. All operations have been carried out in 3D Cartesian coordinates, from initial data to evolution to wave form extraction. The evolutions are carried out with a formulation of Einstein’s equations based on the conformal, trace-free approach developed originally by Shibata and Nakamura [8] and Baumgarte and Shapiro [9], and further tested and developed in [10].

First, we compare the 2D nonlinear (MAGOR) evolutions with the results of the Regge-Wheeler perturbative approach. We consider the nonlinear evolution of a family of data sets with parameters ($Q_0, n' = 3, \eta_0 = 2, \sigma = 1$). For low amplitude cases with $Q_0 < 8$, we are in the linear regime and even the nonlinear evolutions exhibit strongly linear dynamics. In Fig. 1 we show $l = 3$ wave form results obtained from the 2D nonlinear code, for the case $Q_0 = 2$. When we compared with Regge-Wheeler evolutions of the $(\phi, \partial_t \phi)$ system we have found that the agreement was so close that the two curves could not be distinguished in the plot. The perturbative-numerical agreement is equally good with the other linear wave forms at low amplitude so we will leave the perturbative results out of the plots and focus on the transition to nonlinear dynamics. Figure 1 shows the $l = 3$ gauge-invariant Moncrief wave forms for a sequence of such evolutions of increasing amplitude Q_0 . The wave forms have all been nor-

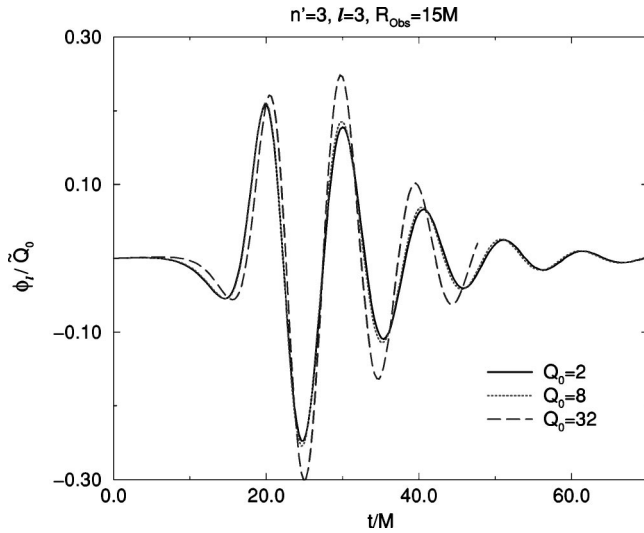


FIG. 1. The $l=3$, odd-parity wave form, extracted at isotropic coordinates $\bar{r}=15M$ from the fully nonlinear 2D evolution code, for a series of evolutions with parameters $(Q_0, n'=3, \eta_0=2, \sigma=1)$. For $Q_0 \leq 8$ the linear regime is maintained, while for $Q_0=32$ nonlinearities are well noticeable. The effect of nonlinear contributions increases the scaled amplitude of the wave form and increases its frequency.

malized by the amplitude factor $\tilde{Q}_0 = Q_0/M^2$ to accentuate nonlinear effects. If the system is in the linear regime, the normalized wave forms will all line up, as is clearly the case in the regime $Q_0 \leq 8$. For the large amplitude case $Q_0=32$, the normalized wave form is much larger, indicating that here we are well into the nonlinear regime.

The wave forms we have shown so far are the only ones predicted to linear order in perturbation theory. We would need to apply higher order perturbation theory to predict wave forms for the even-parity or higher- l odd parity modes. Nevertheless general considerations from the perturbative point of view do provide some expectations on the scaling of the other nonlinear wave form modes within the families considered here. We return to the $n'=3$ family for an example. The leading contribution to the $n'=3$, $l=5$ odd-parity waveform comes from the cubic coupling of the first order $l=3$ odd-parity mode discussed above (including the coupling of the $l=3$ odd-parity mode with the second order even-parity $l=2$ mode expected via the source term contribution to the solution of the Hamiltonian constraint in the initial data). Thus, this wave component should appear at the third perturbative order. We verify this expectation by plotting the numerical results for the $l=5$ odd-parity wave forms scaled this time by \tilde{Q}_0^3 in Fig 2. Although the magnitudes of these wave forms are far smaller than those of the $l=3$ mode we again see very nice agreement, below $Q_0=8$, with the perturbative expectation, that the wave forms should superpose.

Let us now take another look at Fig. 1 to consider what is happening as we move into the nonlinear regime where the wave forms no longer superpose. In the graph we see the same general features arising as begin to drive the system into the nonlinear regime. These are higher frequency ring-

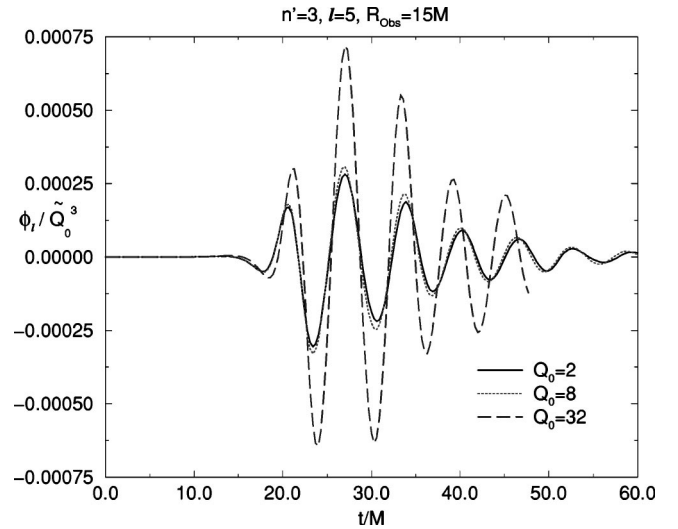


FIG. 2. For $n'=3$, the $l=5$ multipole is generated by cubic products of the odd-parity wave. Still higher nonlinearities switch on for $Q_0=32$ and show the generic increase in the frequency of the wave.

ing, and larger amplitudes for the later parts of the wave form. At $Q_0=32$ the $n'=3$ case shows a roughly 10% increase in frequency. Since the final state of the system will be a black hole, we expect quasi-normal ringing in the late-time behavior of the system regardless of the size of the initial perturbations. This is indeed what we see in the wave forms, except that the ringing is at a higher frequency (relative to the initial mass of the system) than we expected. This indicates that the final ringing black hole has less mass than the ADM mass of the initial data. The perturbations have grown large enough to generate radiation amounting to a noticeable fraction of the total ADM mass leaving behind a slightly smaller black hole. The smaller mass of the final black hole is also consistent with larger amplitudes, since the scaled perturbation $\tilde{Q}_0 = Q_0/M^2$ is larger relative to a smaller mass black hole. The arrival time of the wave pulse is not strongly affected by the change in mass because the time and wave extraction points are both scaled against the initial mass.

Having successfully tested the 2D fully nonlinear code MAGOR for odd-parity distortions against perturbative evolutions, we can now test the 3D code CACTUS against the 2D one. In CACTUS, the initial data are evolved in the full (no octant) 3D mode, with a second order convergence algorithm, maximal slicing, and static boundary conditions. Note we perform the conformal-traceless scheme [10] for this evolution.

The runs presented in Fig. 3 show very nice agreement with the 2D code (hence also with perturbation theory). Note that the spatial resolution ($\Delta x^i = 0.15M = 0.3$) is not high. Here we show wave forms for $t/M \leq 30$. The runs do *not* crash afterwards, but become less accurate due to the low resolution and boundary effects, and even later to collapse of the lapse. The l modes shown in Fig. 3 are essentially dominated (for $Q_0=2$) by the linear initial distortion of the black hole. Those are the modes that we can compare with first

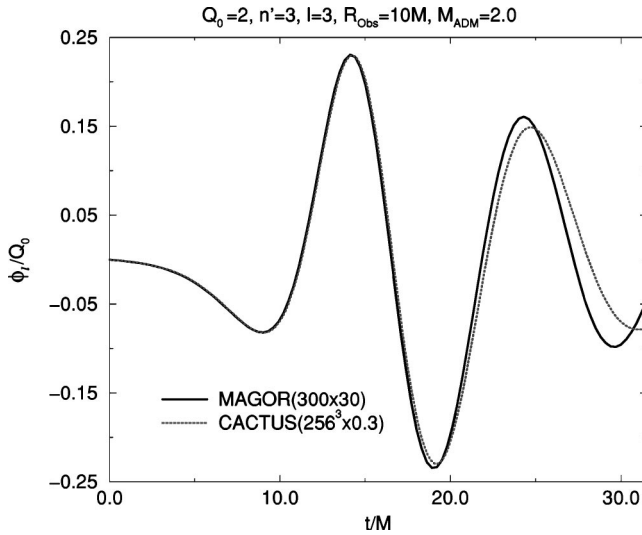


FIG. 3. The $l=3$, odd-parity Moncrief wave form, extracted from the fully nonlinear 3D evolution code CACTUS (dotted line). The spatial grid consists of 256^3 points with a separation of $0.15M$. The ADM mass of the black hole is $M=2.0$ and ($n'=3, Q_0=2, \eta_0=2, \sigma=1$). For comparison we also plot the results of evolving the same initial data with the fully nonlinear 2D evolution code MAGOR (solid line).

order perturbation theory. Since we have two nonlinear codes we can now compare their predictions for modes dominated by nonlinear effects. That is the case of the odd mode $l=5$ when the initial data parameter is $n'=3$. This mode has a linear contribution only for $l=3$. For $l=5$ is easy to see that to generate an odd mode we need at least cubic contributions. Thus this mode will scale as Q_0^3 . To be able to verify the agreement between the 2D and 3D codes we amplified this mode taking $Q_0=32$ and checked the (almost) quadratic convergence of CACTUS to the correct results as shown in Fig. 4. We emphasize that in all plots the agreement among wave forms has been achieved without the aid of any free parameters and thereby stand as a strong verification of these techniques.

Although the distorted black hole initial data configurations we consider here are not necessarily astrophysically relevant, our analysis provides an example of the usefulness of perturbation theory as an interpretive tool for understanding the dynamics produced in fully nonlinear evolutions. In order to distinguish the cases of linear and nonlinear dynamics we simply show the output of the full nonlinear code, but

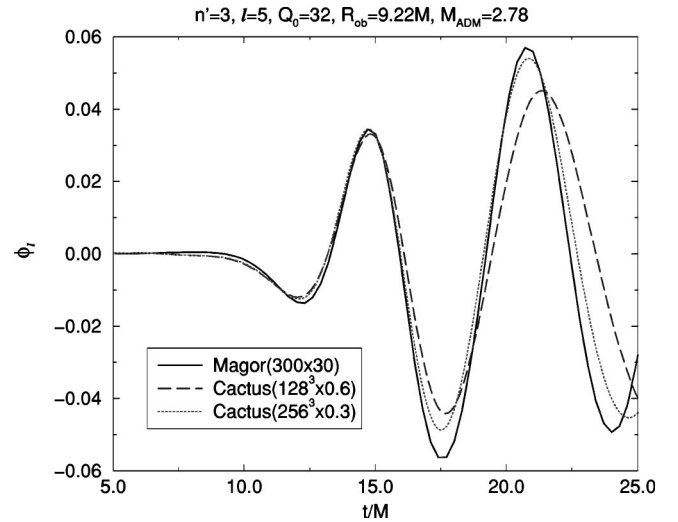


FIG. 4. The $l=5$, odd-parity Moncrief wave form produced by the 3D code CACTUS (dotted line) with initial data having ($n'=3, Q_0=32, \eta_0=2, \sigma=1$) and $M_{ADM}=2.777$. This is a purely nonlinear mode, its leading term being cubic in the amplitude Q_0 . Comparison with the 2D results (solid line) show a good rate of convergence with the grid spacing (from $\Delta x=0.6M/2.777$ to $\Delta x=0.3M/2.777$).

we scale it by the factor Q_0/M^2 so that, if the system is responding linearly to Q_0 all the wave forms will lie exactly on top of one another. Using this procedure we are able to recognize the emergence of nonlinear dynamics. Considering the mixing of perturbative modes also enables us to understand the results of one case which displays strictly nonlinear behavior, the $l=5$ wave form of the initial data with $n'=3$ (see Figs. 2 and 4). This wave strictly vanishes to linear order in \tilde{Q}_0 and scales at lower amplitudes like \tilde{Q}_0^3 . The perspective of perturbation theory allows us to create a full picture, identifying and explaining aspects of the nonlinear dynamics even when the perturbations are beyond the linear regime. In this case we find that linearized dynamics provide a very good approximation of the systems' behavior until the radiation constitutes a significant portion of the initial mass, producing a smaller final black hole and, for example, higher quasi-normal ringing frequencies.

We would like to thank our colleagues at AEI, especially Gabrielle Allen. M.C. holds a Marie-Curie Fellowship (HPMF-CT-1999-00334). The nonlinear computations have been performed on the SGI Origin 2000 at AEI and the Cray T3E at MPI-Garching.

- [1] A. M. Abrahams *et al.*, Phys. Rev. Lett. **80**, 1812 (1998).
- [2] J. Baker, B. Brügmann, M. Campanelli, and C. O. Lousto, Class. Quantum Grav. **17**, L149 (2000).
- [3] G. Allen, K. Camarda, and E. Seidel, gr-qc/9806014.
- [4] S. Brandt and E. Seidel, Phys. Rev. D **54**, 1403 (1996).
- [5] T. Regge and J. Wheeler, Phys. Rev. **108**, 1063 (1957).
- [6] F. J. Zerilli, Phys. Rev. D **2**, 2141 (1970).

- [7] V. Moncrief, Ann. Phys. (N.Y.) **88**, 323 (1974).
- [8] M. Shibata and T. Nakamura, Phys. Rev. D **52**, 5428 (1995).
- [9] T. W. Baumgarte and S. L. Shapiro, Phys. Rev. D **59**, 024007 (1999).
- [10] M. Alcubierre, G. Allen, B. Brügmann, E. Seidel, and W.-M. Suen, gr-qc/9908079 (1999).